nature structural & molecular biology

Inverse coupling in leak and voltage-activated K^+ channel gates underlies distinct roles in electrical signaling

Yuval Ben-Abu[1], Yufeng Zhou[2], Noam Zilberberg[1] & Ofer Yifrach[1]

Voltage-activated (Kv) and leak (K_{2P}) K^+ channels have key, yet distinct, roles in electrical signaling in the nervous system. Here we examine how differences in the operation of the activation and slow inactivation pore gates of Kv and K_{2P} channels underlie their unique roles in electrical signaling. We report that (i) leak K^+ channels possess a lower activation gate, (ii) the activation gate is an important determinant controlling the conformational stability of the K^+ channel pore, (iii) the lower activation and upper slow inactivation gates of leak channels cross-talk and (iv) unlike Kv channels, where the two gates are negatively coupled, these two gates are positively coupled in K_{2P} channels. Our results demonstrate how basic thermodynamic properties of the K^+ channel pore, particularly conformational stability and coupling between gates, underlie the specialized roles of Kv and K_{2P} channel families in electrical signaling.

K^+ channels are pore-forming membrane proteins that open and close in response to changes in chemical or electrical potential, thereby regulating the flow of K^+ ions across biological membranes. This fundamental process underlies the generation of nerve and muscle action potentials[1]. A K^+ ion traversing the membrane through the pore domain of a K^+ channel encounters two structural gates along the ion-conduction pathway: an activation gate at the intracellular entrance to the channel and a distant slow inactivation gate at the extracellular entryway of the channel, at the selectivity filter[2]. This pore design is common to almost all K^+ channels, irrespective of their mode of gating[3–5].

The members of two K^+ channels families, that is, leak or background and voltage-activated channels (K_{2P} and Kv channels, belonging to the dimeric two-pore domain and tetrameric K^+ channel varieties, respectively), have key, yet distinct, roles in electrical signaling. K_{2P} channels are open at all membrane voltages[6,7] and, therefore, are involved in determining the threshold for action potential generation and control action potential firing frequency. Kv channels, on the other hand, are closed at negative membrane voltages and open only upon membrane depolarization[8–10]. Following their opening, Kv channels close either via fast (N-type) or slow (C-type) inactivation gates. The coordinated opening and closing of Kv channel activation and inactivation gates is responsible for modulation of the descending repolarizing phase of the action potential[1].

Despite the common architecture of K^+ channel pores, the distinct physiological roles of Kv and K_{2P} channels in electrical signaling must reflect fundamental differences in the intrinsic thermodynamic properties of their pore domains, in particular in the mode of operation of the pore gates that control the flow of K^+ ions across the membrane. Indeed, several differences in the manner by which the pore gates in Kv and K_{2P} channels operate are known. Whereas gating of the Kv channel pore involves both the lower activation[11,12] and upper slow inactivation[13–18] gates, members of the K_{2P} channel family were reported to open and close solely through their upper gate[19–21]. Furthermore, gating of leak channels has been shown to occur in a manner analogous to the C-type inactivation process of Kv channels, as judged by the coherent effects of changes in external K^+ concentrations, binding of quaternary ammonium blockers, blockage of external bivalent metal ions and mutations on leak channels gating[19–21]. The existence of a lower activation gate in this K^+ channel family, however, has never been demonstrated.

In the Kv channel family, the lower activation and upper slow inactivation pore gates were shown to be coupled[22–25]. Such coupling was demonstrated in both directions: whereas previous work showed that opening of the lower activation gate induces closure of the upper slow inactivation gate[22,23], recent work has shown that upper gate closure promotes lower gate opening[24,25]. It has been suggested that such negative cross-talk provides the means to control the choreographed opening and closing of the respective Kv channels activation and inactivation gates during action potential generation[24]. Considering the roles of leak channels in electrical signaling, in particular the fact that they remain open at all membrane voltages, it is unlikely that a similar gating mechanism is used in this K^+ channel family. Instead, the open leak channel may either not possess a lower activation gate, or, if it does, then the activation and slow inactivation pore gates would be positively coupled, with the opening of the lower activation gate signaling the opening of the upper inactivation gate. Strong positive coupling between the gates, combined with the constitutively

[1]Department of Life Sciences and the Zlotowski Center for Neuroscience, Ben-Gurion University of the Negev, P.O. Box 653, Beer Sheva 84105, Israel. [2]Department of Cellular and Molecular Physiology, Yale University School of Medicine, P.O. Box 208084, New Haven, Connecticut 06520-8084, USA. Correspondence should be addressed to O.Y. (ofery@bgu.ac.il) or to N.Z. (noamz@bgu.ac.il).

Received 8 July; accepted 10 November; published online 21 December 2008; doi:10.1038/nsmb.1525

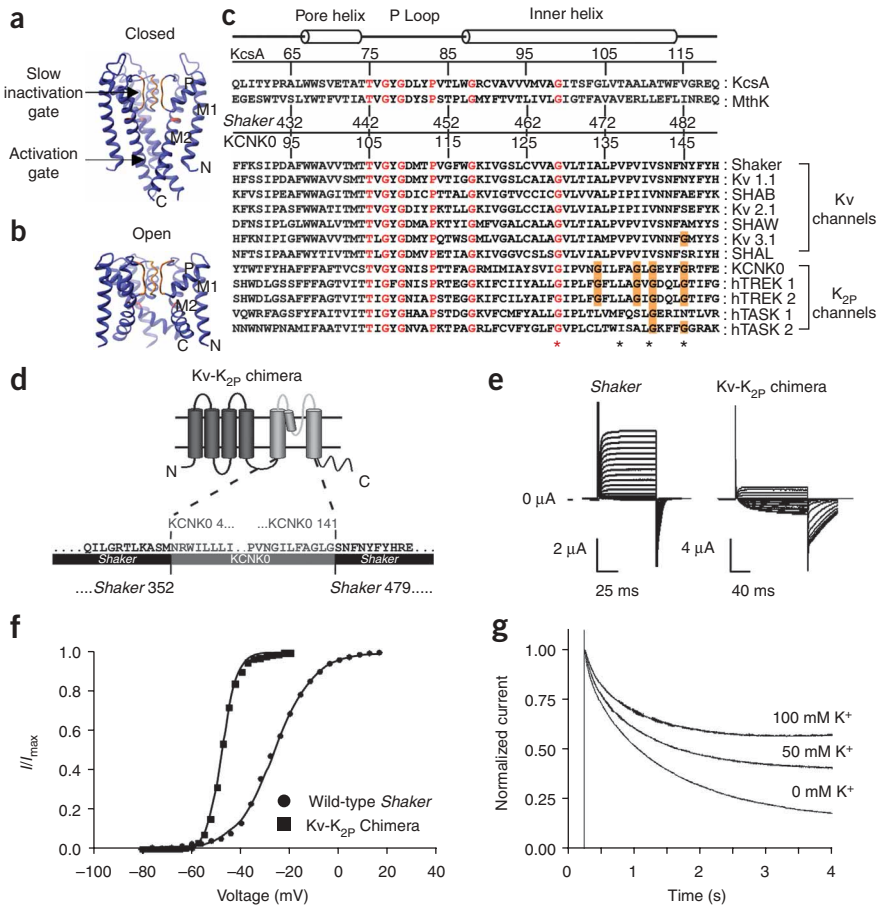

Figure 1 Leak channels contain a lower activation gate. Ribbon representations of the closed (KcsA) (**a**) and open (MthK) (**b**) K^+ channel pore structures with the M1, P and M2 labels denoting the outer, pore and inner helices, respectively. The gating hinge glycine is colored red. (**c**) Multiple sequence alignment of the inner helix region of several voltage-gated and K_{2P} (first pore domain) K^+ channels. Black asterisks indicate the 'hydrophobic seal' positions, as previously defined[35]. The red asterisk indicates the gating hinge glycine position. The four channel positions analyzed in the current study are highlighted in yellow. (**d**) Sequence boundaries of the Kv-K_{2P} chimeric channel protein. (**e**) K^+ currents recorded from *X. laevis* oocytes expressing wild-type or chimeric Kv-K_{2P} channel proteins under two-electrode voltage clamp. (**f**) Voltage-activation curves for the K^+ channels indicated in **e**. Smooth curves correspond to a two-state Boltzmann function. The following values were obtained for the activation midpoints and slopes of wild-type and Kv-K_{2P} channels: $V_{1/2,wt} = -26.0 \pm 0.2$ mV; $Z_{wt} = 3.2 \pm 0.1$; $V_{1/2\ Kv\text{-}K2P,} = -49.5 \pm 0.1$ mV; $Z_{Kv\text{-}K2P} = 8.0 \pm 0.1$. (**g**) Scaled macroscopic K^+ currents through the Kv-K_{2P} chimeric channel, measured under a prolonged depolarizing pulse of 60 mV in the presence or absence of different external K^+ ion concentrations. Steady-state slow inactivation levels (in percentages) of 87.8 ± 2.7, 61.2 ± 2.4 and 36.7 ± 4.5 were obtained in the presence of 0, 50 and 100 mM external K^+ concentrations ($n = 7$), respectively.

open nature of the activation gate, would thus ensure that efficient and constant K^+ leak currents traverse the membrane. Here we examine these possibilities.

RESULTS

Leak channels possess a lower activation gate

To compare the gating properties of leak K_{2P} and Kv channels, we made use of the respective prototypical KCNK0 and *Shaker* channels of *Drosophila melanogaster*. In referring to the inherent modularity of K^+ channels, in the case of the Kv channel we used a *Shaker* 'wild-type' variant lacking the N-terminal inactivation ball-and-chain domain[26,27], whereas in the case of the leak channel we used a 'wild-type' KCNK0 variant in which the C-terminal regulatory domain is truncated (KCNK0-ΔC), but the normal channel gating pathway is preserved[20,28]. As will be evident in the following, just as the truncation of the modular inactivation ball-and-chain domain of Kv channels led to profound understanding of the activation pathway of the channel[29–32], the use of this reductionist approach in the case of the KCNK0 leak channel is expected to yield valuable information with respect to the fundamental principles underlying its gates' movements.

The pore domains of Kv and K_{2P} channel family members demonstrate opposing intrinsic conformational stability phenotypes. In the prototypical *Shaker* Kv channel, systematic energetic perturbation analysis suggests that the closed state of the pore is optimally packed and, therefore, intrinsically more stable than the open state[33]. By contrast, the open pore conformation is intrinsically more stable in the prototypical 'wild-type' KCNK0 leak channel[20]. This essential difference in conformational stability between the two channel pores may in turn reflect differences in the status of their activation gates. Thus, whereas the *Shaker* channel activation gate prefers the closed conformation, with its inner helices crossed (as reflected in the KcsA structure[2], **Fig. 1a**), the activation gate of the leak K^+ channel, should it exist, would be predominantly open, with its inner helix bundle-crossing permanently spread apart (as in the MthK structure[34]; **Fig. 1b**).

Marked sequence differences in the activation gate regions of the Kv and K_{2P} channel families (**Fig. 1c**) offer support for this assertion. Whereas the activation gate region of Kv channel family members is mostly spanned by hydrophobic residues, the corresponding region of K_{2P} channel family members, the predicted site of a putative activation gate, is lined by several glycine residues (**Fig. 1c**). In particular, two of the three residue positions (111 and 115, KcsA numbering), invariably hydrophobic in many K^+ channel families and termed 'hydrophobic seal' residues[35], are primarily glycines in the leak K_{2P} channels. As such, the presence of glycines along the leak putative channel activation gate may affect hydrophobic contacts at the bundle crossing, or have other consequences on channel gating, stemming from side chain size, packing or flexibility (refer to ref. 36 for a thorough discussion of the role of glycines in K^+ channel function). Could the presence of glycines at the putative leak channel activation gate be responsible for the predominantly open nature of its pore domain?

The question posed above implies that K_{2P} channels contain a constitutively open lower activation gate. However, for a channel to possess a functional gate, its ability to open and close must be demonstrated. To this end, we designed a chimeric channel protein in which the first pore domain of the predominantly open KCNK0 channel (open probability (P_o) of ~0.8 (ref. 20)) was fused to the voltage-sensor domain of the *Shaker* Kv channel (**Fig. 1d**) (Methods).

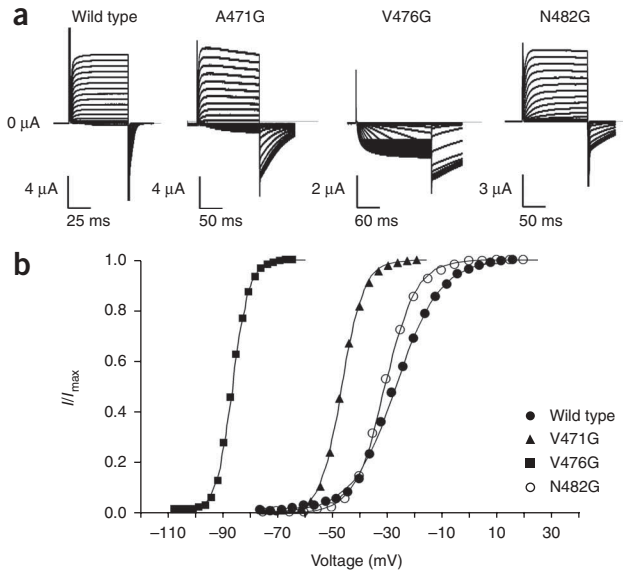

Figure 2 Mutations of hydrophobic residues in the activation gate to glycine stabilize the open state of the *Shaker* channel. (**a**) K^+ currents recorded from *Xenopus laevis* oocytes expressing wild-type or mutant *Shaker* channels under two-electrode voltage clamp. (**b**) Voltage-activation curves for the K^+ channels indicated in **a**. Smooth curves correspond to a two-state Boltzmann function. The following values were obtained for the activation midpoints and slopes of the mutant channels: $V_{1/2,\ A471G} = -46.0 \pm 0.08$ mV; $Z_{A471G} = 6.5 \pm 0.1$; $V_{1/2,\ V476G} = -86.0 \pm 1$ mV; $Z_{V476G} = 8.9 \pm 0.1$; $V_{1/2,\ N482G} = -32.0 \pm 0.\ 1$ mV; $Z_{N482G} = 4.5 \pm 0.1$.

In such a chimera, should the voltage-sensor domain force the KCNK0 channel pore to shut in a voltage-dependent manner, then strong evidence for the ability of the putative leak channel activation gate to close would be offered. Initially, the chimeric Kv-K_{2P} channel boundaries were chosen so as to include the Kv channel regions reported as essential for normal voltage-dependent opening of the lower activation gate, namely the so-called S4-S5 linker and the post-S6 region[3,37]. These optimal boundaries, derived from elaborate study of the gating properties of several different *Shaker*-KcsA chimeric proteins[37], did not, however, yield a functional Kv-K_{2P} channel (not shown). By contrast, a second chimeric Kv-K_{2P} channel, the boundaries of which encompass the entire putative activation gate region of the KCNK0 channel (**Fig. 1d**), expressed functional K^+ currents in a manner typical of a voltage-dependent channel (**Fig. 1e**).

Figure 1f presents voltage-activation relations of the chimeric channel, demonstrating a monophasic gating transition from the closed to open state. The midpoint voltage of the Kv-K_{2P} activation curve is shifted to the left along the voltage axis by –35 mV, as compared to the wild-type *Shaker* channel. We calculated an open-state stabilization effect of 7.2 (± 0.1) kcal mol^{-1} for the chimeric channel protein (Methods), seemingly reflecting the opposing intrinsic conformational stability phenotypes of the *Shaker* and KCNK0 K^+ channel pores.

Although the voltage-dependent opening of the Kv-K_{2P} chimeric channel occurs on the millisecond timescale, characteristic of activation gate movements, one cannot rule out the possibility that the KCNK0 gate that is open is, in fact, the upper slow inactivation gate. To address this issue, we measured chimeric channel activation using a prolonged depolarizing pulse, on a timescale typical for the onset of C-type inactivation. Under these conditions, the voltage sensor–attached KCNK0 pore indeed inactivates in a manner characteristic of a C-type inactivating Kv channel, as judged by the effect of increasing external K^+ ion concentrations (**Fig. 1g**) and tetraethylammonium (TEA) (data not shown) on the steady-state levels of C-type inactivation in the Kv-K_{2P} chimera. These results argue that the voltage-dependent opening of the Kv-K_{2P} chimera, observed in the short millisecond timescale (**Fig. 1e**,**f**), reflects lower activation gate movements.

To summarize, our results on the Kv-K_{2P} chimera demonstrate the ability of the open KCNK0 pore to close, probably by a forcing, through the actions of the voltage-sensor domains, of its inner helices to assume the crossed bundle, closed structure of the activation gate. In the case of the wild-type KCNK0 channel, this gate is presumably essentially open (see below).

Activation gate residues determine the pore's stability

We next examined channel gating effects obtained upon replacing activation gate amino acid residues in one channel with the corresponding residues from the second channel. Attention primarily focused on those hydrophobic positions in the Kv channel family that mostly correspond to glycines in the leak K^+ channels. Accordingly, we systematically measured the effects on voltage-dependent gating realized upon individually mutating four S_6 positions (that is, residues 471, 476, 478 and 482) of the *Shaker* Kv channel—residues found at, or near, the activation gate—to glycines. Mutation of the hydrophobic residues at positions 471 and 476 to glycine resulted in a dramatic open-state stabilization, reflected in the slow closure rates of the two mutants, following membrane depolarization (**Fig. 2a**), and in the voltage dependence of channel opening (**Fig. 2b**). The A471G and V476G mutant channels reached half-maximal activation at around –50 and –85 mV, respectively, whereas the wild-type channel did not reach half-activation until nearly –25 mV (**Fig. 2b**). The activation curve of the *Shaker* V478G crossover mutant could not be obtained, owing to the extremely low K^+ currents expressed. However, it was previously demonstrated that larger hydrophobic replacements for Val478 at this second 'hydrophobic seal' position of the *Shaker* channel resulted in stabilization of the channel closed conformation[38]. Finally, the activation curve of the N482G mutant resembled that of the wild-type channel.

We also performed complementary experiments, in which the glycine residues of the activation gate of the KCNK0 K_{2P} channel were replaced by the corresponding hydrophobic amino acids of the *Shaker* channel. The G134A, G139V and G141V KCNK0 mutants expressed lower K^+ currents than did the wild-type or mutant G145N channels (**Fig. 3a**). The reduced K^+ current levels observed for the G134A, G139V and G141V KCNK0 activation gate mutants (**Fig. 3b**) could reflect a reduction in the open probability of the channel (P_o), in single-channel conductance or in cell-surface expression of the channel.

To distinguish between these possibilities, we carried out cell-attached single-channel recordings of the wild-type and mutant KCNK0 channels (**Fig. 3c**). As can be clearly seen, all of the hydrophobic KCNK0 mutants, apart from G145N, revealed a dramatic reduction in open channel probability, as compared to the predominantly open wild-type channel. It should be noted that the KCNK0 channel does not present the single-channel recordings characteristic of a C-type inactivating voltage-dependent K^+ channel, that is, where the probability of channel opening decays with time. This is because the leak channel under study is voltage independent. Therefore, the open probability of the leak channel does not change during the course of our measurement and thus reflects the steady-state conformational stability of the pore. Unitary

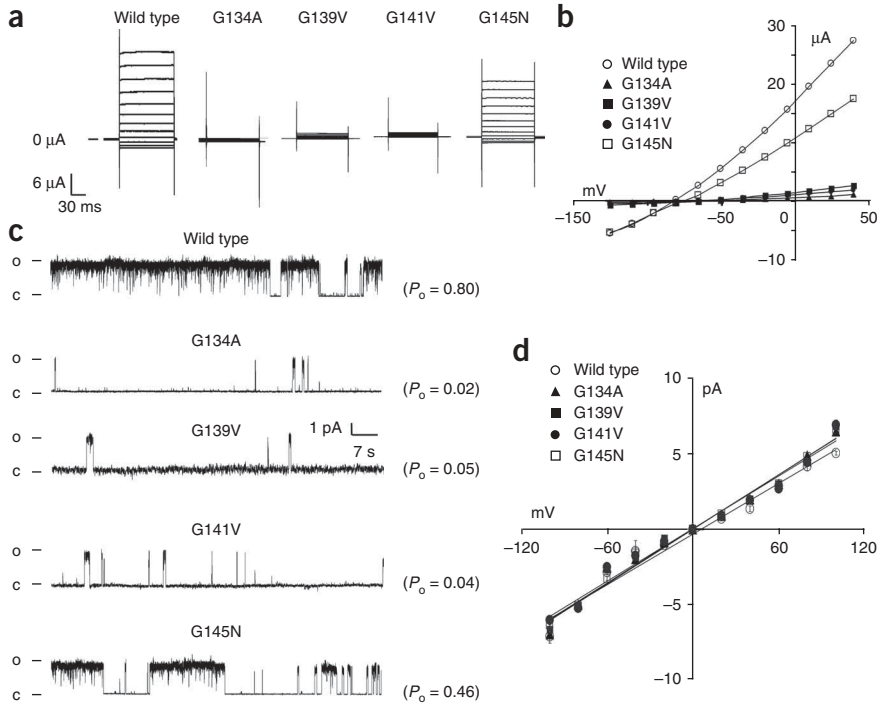

Figure 3 Mutations of glycine residues in the activation gate to hydrophobic residues result in a reduction in the open probability of the KCNK0 leak channel. (**a**) K^+ currents recorded from *X. laevis* oocytes expressing wild-type or mutant KCNK0 leak channels under two-electrode voltage clamp (Methods). (**b**) Current-voltage (*I/V*) curves for the channels indicated in **a**. (**c**) Representative cell-attached single-channel recordings of the channels indicated in **a** measured at 60 mV, with 140 mM K^+ solution in the pipette. Traces were sampled at 20 kHz and were filtered at 0.1 kHz for presentation clarity. The presented traces are only short segments of typically 10-min or longer single-channel recordings from membrane patches bearing only one wild-type or mutant channel. The open (O) and closed (C) currents levels are indicated. Open probabilities for wild-type or mutant leak channels are reported. (**d**) Unitary conductance measurements for the channels indicated in **a**, under symmetric conditions.

I-V curves for all of the mutants revealed no changes in single-channel conductance[20] (**Fig. 3d**).

Our single-channel recording data thus reveal that the reduction in current-level expression upon mutation, observed in the whole-cell current measurements (**Fig. 3b**), is a reflection of a dramatic decrease in the open probability of the mutant channels. Although additional effects on KCNK0 channel maturation and cell-surface expression resulting from mutation cannot be ruled out, they would be minor and would not weaken the conclusion reached above. The results obtained upon mutation of the third 'hydrophobic seal' position in either channel (that is, N482G or G145N, *Shaker* or KCNK0 numbering, respectively) are consistent with this position lying beyond the activation gate region of either channel[12]. Taken together, our results for both the *Shaker* and KCNK0 channels are coherent and imply an important role for three of the four activation gate positions analyzed in determining the intrinsic conformational stability of the K^+ channel pore domain.

Cross-talk between the activation and slow inactivation gates of leak K^+ channels

The reduction in the open probability of the KCNK0 channel observed upon replacement of the activation gate glycine with a hydrophobic residue is compatible with the ability of the lower activation gate to close, in particular when considering the coherence of this observation with the gating effects of the corresponding Kv channel mutants. Alternatively, such reduction could originate, entirely or in part, from closure of the upper slow inactivation gate, despite these mutations being localized to the lower activation gate.

To test this latter possibility, we exploited the fact that Zn^{2+} ions exclusively bind to the closed conformation of the KCNK0 channel slow inactivation gate, thus serving as a reliable probe of this state[20]. If the reduction in current-level expression observed with the KCNK0 activation gate mutants indeed results from closure of the slow inactivation gate, then this should be reflected by an increased rate of K^+ current blockage by Zn^{2+} relative to the wild-type channel[20]. As predicted, all KCNK0 activation gate mutants, apart from G145N, were blocked by Zn^{2+} on a much faster timescale than was the wild-type channel (**Fig. 4a**,**b**). Stabilization of the closed conformation of the slow inactivation gate was further manifested in the dose-response curves of the mutant K^+ currents realized upon blockage by Zn^{2+} (**Fig. 4c**). As shown in **Figure 4d**, K_C^I, the equilibrium constant for inactivation gate (I) closure ($K_C^I = [I_c]/[I_o]$), obtained upon fitting of the data to an equation based on the reaction scheme indicated in the legend to **Figure 4c**, is dramatically increased for all KCNK0 mutants but G145N, reflecting stabilization of the closed conformation of the inactivation gate. Our findings thus indicate that those KCNK0 activation gate mutants that presumably induce lower activation gate closure also stabilize the upper slow inactivation gate in its closed conformation, explaining, at least in part, the reduction in the open probability of the mutant channels.

The results presented above imply that the lower activation and upper slow inactivation gates of KCNK0 are coupled. Nonetheless, direct evidence showing that the KCNK0 mutants affect the status of the lower activation gate remains elusive. How then can one dissect the contribution of each gate to the observed reduction in open probability? To address this question, we introduced the G139V and G141V activation gate mutants into the background of an inactivation-abolished, constitutively open ($P_o = 1$) KCNK0 mutant (G134D; see **Supplementary Results** online). Both the G134D G139V and the G134D G141V KCNK0 double mutants expressed K^+ currents to a lower extent than did the G134D channel (**Fig. 5a**). This, again, implies a reduction in the open probability of the G134D channel upon the introduction of mutations at the activation gate, as indeed revealed by single-channel recordings of the double mutants (**Fig. 5b**). This time, however, the reduction in the open probability of the channel did not originate from facilitating closure of the upper slow inactivation gate upon mutation because, as with the G134D mutant channel (**Supplementary Results**), the G134D G139V and G134D G141V KCNK0 double mutants showed no blockage by Zn^{2+} ions (compare **Figures 5c** and **4a**). We therefore conclude that, for these double mutants, reduction in the open probability of the channel results exclusively from stabilization of the closed conformation of the lower activation gate, thus further supporting the existence of a lower activation gate in the KCNK0 leak channel.

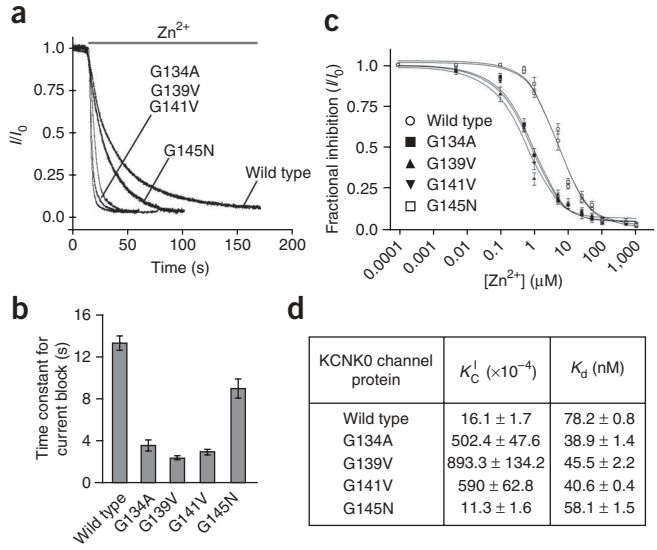

KCNK0 channel protein	K_C^I ($\times 10^{-4}$)	K_d (nM)
Wild type	16.1 ± 1.7	78.2 ± 0.8
G134A	502.4 ± 47.6	38.9 ± 1.4
G139V	893.3 ± 134.2	45.5 ± 2.2
G141V	590 ± 62.8	40.6 ± 0.4
G145N	11.3 ± 1.6	58.1 ± 1.5

Figure 4 Hydrophobic activation gate mutants of the KCNK0 leak channel induce closure of the upper inactivation gate. (**a**) The effects of Zn^{2+} (100 μM) on K^+ current levels in oocytes expressing wild-type or mutant KCNK0 channels (Methods). (**b**) Time constants of current blockage for wild-type and mutant channels presented in **a**, calculated by fitting the data to a single exponential equation (Methods). Error bars represent s.e.m. (**c**) Dose-response for Zn^{2+}-mediated inhibition of wild-type and mutant KCNK0 channels indicated in **a**. Smooth curves correspond to an equation derived on the basis of the scheme $I_O \overset{K_C^I}{\longleftrightarrow} I_C + Zn^{2+} \overset{Kd}{\longleftrightarrow} I_C Zn^{2+}$, where I_O and I_C are the respective open and closed conformations of the inactivation gate (see data analysis section in Methods). Values for the equilibrium constants of activation gate closure ($K_C^I = [I_c]/[I_o]$) and Zn^{2+} binding to the closed inactivation gate (K_d) of the wild-type or mutant channels are listed in **d**. Essentially, similar K_d values were obtained for Zn^{2+} binding to the different mutants, confirming the usefulness of Zn^{2+} as a reporter of the closed status of the slow inactivation gate[21].

The above conclusion is further supported, in a direct manner, by whole-cell K^+ current blockage experiments using Ba^{2+} as an open-state blocker[39]. In such experiments, Ba^{+2} ions are applied to the intracellular side of the channel upon injection into oocytes expressing the mutant KCNK0 channels (Methods). Access of Ba^{2+} ions to their binding site at the inner vestibule of the channel is possible only when the lower activation gate of the channel is opened. As can be seen in **Figure 5d**, the kinetics of Ba^{2+}-induced K^+ current blockage is much slower in the case of oocytes expressing the G134D G139A and G134D G141A activation gate double mutants, as compared to the G134D KCNK0 channel. This outcome is expected, considering the marked reduction in the open probability of these double-mutant channels (**Fig. 5b**), reflecting stabilization of the closed conformation of the activation gate upon mutation. The dramatic reduction in the mean open time observed for these double-mutant channels (**Fig. 5b**) dictates restricted access of Ba^{2+} ions to their site of interaction and, therefore, results in slower blockage kinetics. The similar time constants for the Ba^{2+}-induced current blockage obtained for both double mutants (**Fig. 5e**), with similar probabilities of channel opening (**Fig. 5b**), suggests that there is a linear correlation between the time constant for Ba^{2+}-induced current blockage and the open probability of the mutant channels, thus further strengthening our assertion for the existence of the lower gate in leak channels and testifying to the reliability of the experimental setup used. To summarize, the results described in this section reveal that both activation and slow inactivation gates of the KCNK0 channel close upon the introduction of hydrophobic replacements at the activation gate, suggesting that both gates are coupled.

A unified gating scheme explains observations made on both K^+ channel families

The prominent conformational stability difference between the pore domains of Kv and leak K_{2P} channel families reflects differences in the operation of the lower activation (A) and upper slow inactivation (I) pore gates. In particular, these differences affect their probabilities of being open (O) or closed (C), as reflected in the thermodynamic gating cycle presented in **Figure 6**, suggested previously[24]. The cycle describes, in a simple reductionist manner, the four possible pore channel states, namely when both gates are closed (A_CI_C state), when either gate is open (A_OI_C and A_CI_O states) or when both gates are open (A_OI_O state).

In the case of the Kv channel family, where the closed pore conformation is intrinsically more stable, the A_CI_O state is the resting conformation. Upon membrane depolarization, the $A_CI_O \rightarrow A_OI_O \rightarrow A_OI_C$

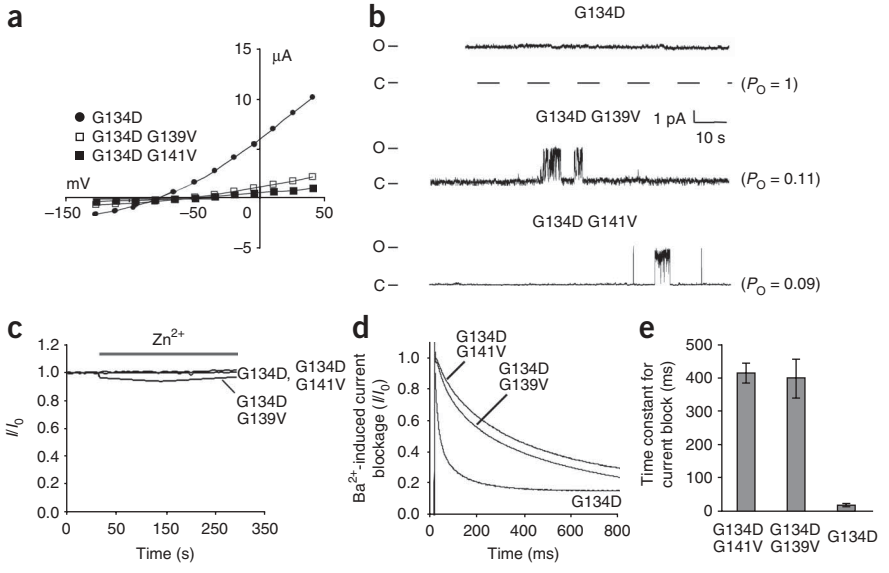

Figure 5 Hydrophobic activation gate mutants of the KCNK0 leak channel induce closure of the lower activation gate. (**a**) Current-voltage (*I/V*) curves for the G134D KCNK0 channel or the G134D G139V and G134D G141V double mutants. (**b**) Representative cell-attached single-channel recordings of the leak channels indicated in **a** (Methods). Traces were sampled at 20 kHz and filtered at 0.1 kHz for presentation clarity. Open probabilities for the different leak channel mutants are indicated. (**c**) K^+ current inhibition for the KCNK0 channels indicated in **a** upon extracellular application of 100 μM Zn^{2+}. (**d**) Inhibition of K^+ current through the KCNK0 channels indicated in **a** upon intracellular application of 250 μM Ba^{2+} (Methods). Ba^{2+}-induced current blockage was initiated by a depolarizing pulse to +40 mV from a holding potential of –80 mV. (**e**) Time constant of Ba^{2+}-induced current blockage (averaged values are reported, $n = 8$–12) for the mutant channels indicated in **a**. Error bars represent s.e.m.

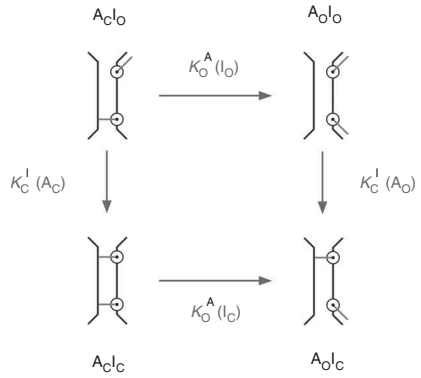

Figure 6 A simplified schematic thermodynamic cycle connecting the four possible K^+ channel pore states, where the lower activation (A) and upper slow inactivation (I) pore gates are either closed (C) or open (O). The four A_CI_O, A_OI_O, A_OI_C and A_CI_C states (see main text), positioned at the corners of the cycle, are composite states each representing the many conformational states usually associated with that state[24]. Horizontal transitions represent activation gate opening (or closing), once with the inactivation gate open ($A_CI_O \rightarrow A_OI_O$ transition) and once with it closed ($A_CI_C \rightarrow A_OI_C$ transition). Similarly, vertical transitions represent closure (or opening) of the upper inactivation gate when the other gate is either closed ($A_CI_O \rightarrow A_CI_C$) or open ($A_OI_O \rightarrow A_OI_C$). The equilibrium constants of the four gating transitions indicated above are denoted by $K_O^A(I_O)$, $K_O^A(I_C)$, $K_C^I(A_C)$ and $K_C^I(A_O)$, respectively. From symmetry considerations along a closed thermodynamic cycle, $K_O^A(I_O) \cdot K_C^I(A_O) = K_C^I(A_C) \cdot K_O^A(I_C)$. Arrows were drawn according to the definition of the gating transitions but all represent equilibrium transitions.

activation-inactivation gating sequence ensues. By contrast, in leak channels, for which the open pore conformation is intrinsically more stable, the A_OI_O state is the resting conformation and gating is described by the vertical $A_OI_O \rightarrow A_OI_C$ inactivation gating transition. For this channel family, the ratio of equilibrium constants is such that, in practical terms, the A_CI_C and A_CI_O states are not populated. The activation gate of the leak channel pore, therefore, has evolved to be predominantly open.

Considering the scheme above, we argue that, in contrast to the behavior of the native KCNK0 leak channel, where gating ensues practically via the $A_OI_O \rightarrow A_OI_C$ transition, for the G139V and G141V activation gate mutants gating occurs predominantly through the $A_CI_O \rightarrow A_CI_C$ parallel inactivation gating transition (**Fig. 6**). This assertion is based on the observation that these mutant channels are more difficult to open (**Fig. 3**), owing to closure of both the activation (**Fig. 5**) and slow inactivation (**Fig. 4**) gates, as described by the $A_OI_O \rightarrow A_CI_O$ and $A_CI_O \rightarrow A_CI_C$ gating transitions, respectively. Evidence for the first of these transitions resulting from mutation originates from separately introducing glycine-to-valine mutations at positions 139 and 141 on the background of the inactivation-abolished G134D mutant, a channel protein locked in the A_OI_O open state. The marked reduction in open probability observed for these double mutants (**Fig. 5**), combined with their insensitivity to blockage by Zn^{2+}, suggests that the activation gate indeed closes. If the leak channel single activation gate mutants were to affect only closure of the activation gate by stabilizing the A_CI_O state, then the $A_OI_O \rightarrow A_OI_C$ inactivation gating transition would be expected to decrease, owing to depletion of the A_OI_O state. The fact that, for these activation gate mutants, the inactivation process is also facilitated, as indicated by the increased sensitivity of the single mutants to Zn^{2+} blockage, points to the presence of the A_CI_C state, resulting from an $A_CI_O \rightarrow A_CI_C$ transition. Therefore, the A_OI_O pore state is depleted upon introducing mutations at the activation gate (P_o changes from $\sim$0.8 to even lower than 0.01, as the reported low P_o values obtained for these mutants (**Fig. 3**) are upper bounds for the true values), whereas the A_CI_C state, in which both gates are closed, accumulates.

DISCUSSION

In the current manuscript, we have compared sequence, structural and functional data of leak and Kv channel families. We noted that, in the case of the K_{2P} channel family, the predicted site of a putative activation gate is lined by several glycine residues (**Fig. 1c**). This is in marked contrast to the hydrophobic residues found in the corresponding positions of Kv channel family members, thus suggesting that the activation gate region has an important role in determining the opposing open and closed intrinsic pore conformational stability phenotypes of K_{2P} and Kv channels, respectively. Cross-mutating, one by one, the glycine activation gate residues of the KCNK0 channel with the corresponding hydrophobic residues of the *Shaker* Kv channel caused a reduction in the open probability of the channel, compatible with the ability of the lower activation gate of KCNK0 to close (**Fig. 5**). Consistent with these results, replacement of hydrophobic residues with glycine at the corresponding positions of the *Shaker* channel facilitated the opening of the lower activation gate, as judged by the marked open state–stabilization effects realized upon mutations. The coherent gating effects of leak and Kv channel activation gate mutants suggest that the movements underlying the closure and opening of the leak channel activation gate, respectively, occur via assembly and disassembly of the inner helices bundle crossing, as suggested for other K^+ channels[34,36,40]. Taken together, our results reveal the existence of a lower activation gate in a K^+ leak channel family member. This assertion is further supported, in a direct manner, by the results of the Ba^{2+} accessibility measurements and when considering the ability of the *Shaker* channel voltage-sensor domain to close shut, in a typical voltage-dependent manner, the activation gate of the KCNK0 channel (**Fig. 1e**,**f**).

Our observation that closure of the lower activation gate upon mutation is accompanied by closure of the upper gate as well (**Fig. 4**) further implies that there is coupling between the activation and slow inactivation gates of leak channels, as is the case for Kv channel family members[24,25]. One can thus ask whether leak and Kv channels have similar modes of coupling between their activation and slow inactivation gates. This question may be answered by considering the unified gating cycle presented in **Figure 6**. This gating cycle is actually a thermodynamic double-mutant cycle[41–43] that can serve as a framework for understanding the nature (whether positive or negative) and magnitude ($\Omega_{coupling}$) of coupling between the activation and slow inactivation gates in K^+ channels (**Supplementary Discussion** online). A 'mutation' in such analysis corresponds to the opening of the activation gate ($A_C \rightarrow A_O$ horizontal transitions) or closing of the inactivation gate ($I_O \rightarrow I_C$ vertical transitions). The equilibrium effect of either 'mutation' is evaluated once when the other gate is closed and a second time when it is open (parallel gating transitions in **Figure 6**). If the two pore gates operate independently, then closure of the slow inactivation gate, for example, would not depend on whether the activation gate is open or closed ($\Omega_{coupling} = K_C^I(A_C)/K_C^I(A_O) = 1$, the additive case; **Supplementary Discussion**). Otherwise, the pore gates can be considered as being coupled ($\Omega_{coupling} \neq 1$).

In the case of the *Shaker* Kv channel, an elegant study[24] demonstrated that the two pore gates are negatively coupled. Opening of the lower activation gate was found to facilitate closure of the inactivation

gate ($K_C^I(A_O) > K_C^I(A_C)$; **Fig. 6**). Although not precisely determined, a $\Omega_{coupling}$ value lower than 1, typical for cases of negative coupling (**Supplementary Discussion**), was implied for this Kv channel system[24]. Our results on the KCNK0 leak channel tell us that, for this K^+ channel family, the two pore gates are instead positively coupled, such that opening (or closing) of the activation gate stimulates the opening (or closing) of the upper inactivation gate (that is, $K_C^I(A_C) > K_C^I(A_O)$; note that the inactivation equilibrium constants are defined in the closing direction (**Fig. 6**)). First, our finding that closure of the lower activation gate of the channel upon mutation further induced closure of the upper inactivation gate points to the two gates being positively coupled. Second, $\Omega_{coupling}$ values of 55.5 (± 19.0) and 36.6 (± 16.0) were calculated for the G139V and G141V mutants when comparing the equilibrium constants of slow inactivation gate closure of wild-type and mutant channels (**Fig. 4d**), reflecting $A_OI_O \rightarrow A_OI_C$ and $A_CI_O \rightarrow A_CI_C$ parallel gating transitions, respectively (**Fig. 6**). Values for $\Omega_{coupling}$ greater than 1 are hallmarks of positive coupling between the gates in the double-mutant gating cycle. The reported $\Omega_{coupling}$ values are, moreover, the lower bounds for the magnitude of positive coupling between the gates, as, for the KCNK0 channel mutants, the equilibrium constant for the $A_OI_O \rightarrow A_OI_C$ transition is of a much lower magnitude than for the wild-type channel. It seems, therefore, that in Kv channels, negative coupling between the gates ensures the adoption of more stable asymmetric pore states, where only one of the gates is open (that is, either the resting A_CI_O or inactivated A_OI_C state). For leak K^+ channels, positive coupling between the gates ensures that more stable symmetric pore states are assumed when both gates are open (the A_OI_O state) or when both gates are closed (A_CI_C), as revealed here upon mutation.

The distinct thermodynamic pore properties of the *Shaker* Kv and KCNK0 K_{2P} channels reflect the different physiological roles of members of these K^+ channel families. To fulfill its role in setting the resting membrane potential close to the *Nernst* potential for K^+ ions, the pore domain of leak K^+ channels needs to be constantly open, ensuring the maintained leak of K^+ current across the membrane. This would be efficiently achieved only if both pore gates evolved to be positively coupled, that is, that at all membrane voltages, the two pore gates are open at the same time. The activation gate of the leak channel, evolved to remain predominantly open, would thus signal the opening of the upper inactivation gate. In Kv channels, where coordinated opening and closing of both the activation and slow inactivation pore gates, respectively, modulates action potential shape and frequency[44–46], negative coupling between the two gates would prime the upper inactivation gate to close as soon as the lower activation gate opens. Thus, the vast repertoire of action potential shapes and patterns that occur in different excitable cells and tissues may reflect not only differences in the activation and inactivation kinetics of the different K^+ channels involved, but also differences in the magnitude[24] and mode of coupling between the activation and inactivation pore gates.

We were intrigued about the possible molecular explanation for the observed inverse modes of coupling in Kv and leak channels. A first hint for such an explanation may arise from the interesting observation that, when measured on a longer timescale typical for the onset of C-type inactivation, the rationally designed Kv-K_{2P} voltage-dependent chimera shows negative coupling between the pore gates, as in normal Kv channels (**Fig. 1g**). This preliminary observation, although requiring further investigation, is in line with other studies on Kv channels reporting that, following activation gate opening, the onset of upper gate closure, and hence negative coupling between the gates, is a result of ensuing mutual structural rearrangements between the voltage-sensor and pore domains[16,47–49].

To summarize, we have demonstrated the existence of a lower activation gate for the leak K^+ channel family, evolved to be predominantly open. Moreover, we have shown that the coupling between the activation and slow inactivation gates of leak channels is inverse to that coupling previously shown for Kv channels[24,25]. The detailed molecular explanation for this difference and the effect of the leak channel regulatory domain on the coupling of both gates still require further investigation. Nonetheless, our results suggest how differences in basic thermodynamic pore properties, in particular intrinsic conformational stability and modes of coupling between activation and inactivation gates (a thermodynamic linkage relation), underlie the distinct roles of Kv and leak K^+ channels in electrical signaling.

METHODS

Molecular biology. In this study, we used the *Shaker-IR* Kv channel variant (N-type inactivation region (residues 6–46) removed) and a K_{2P} KCNK0 variant lacking the channel-regulatory domain (residues 299–1001), but preserving the normal channel-gating pathway[20,28]. mRNA for wild-type or mutant *Shaker* and KCNK0 K^+ channels was synthesized using T7 RNA polymerase, as previously described[33]. Mutations were introduced by the QuickChange method (Stratagene) and confirmed by DNA sequencing of the entire cDNA. The Kv-K_{2P} chimeric channel gene was constructed by blunt-end ligation of two PCR-amplified DNA fragments: an insert containing a phosphorylated DNA fragment of the KCNK0 channel pore domain at the chosen boundaries (**Fig. 1d**) and a template fragment containing the entire sequence of the *Shaker* Kv channel gene, apart from the pore domain, along with the pBluscript plasmid sequence.

Electrophysiology. We recorded K^+ currents from the *Shaker-IR* channel under conditions of two-electrode voltage clamp 1–2 d after wild-type or mutant mRNA injection, as described previously[33]. Briefly, currents were elicited by various depolarization strengths from holding voltages of –110 mV for the V476G mutant and –85 mV for wild-type, N482G and A471G channels. Tail potential was similar to the holding potential. Voltage-activation curves were obtained using the measured tail currents and represent average recordings from 8–10 different oocytes, each measured three times. K^+ currents through the KCNK0 channel were elicited by various depolarization strengths from a holding voltage of –80 mV for 200 ms, as described previously[20]. Oocyte membrane potential was stepped from –125 to + 40 mV in 15 mV increments. The bath solution contained 93 mM NaCl, 4 mM KCl, 1 mM $MgCl_2$, 0.3 mM $CaCl_2$, 5 mM HEPES, pH 7.4. Oocytes were injected with 5 ng of wild-type or mutant cRNA and measured at the same time range 1–3 d after injection, using a Geneclamp 500 Amplifier and pCLAMP 9.0 acquisition software (Axon, Molecular Devices). Current-voltage relations of the wild-type or mutant KCNK0 channels were generated using five to eight oocytes. Reversal potentials of K^+ currents in the wild-type or the various KCNK0 mutants were determined in external K^+ concentrations of 4, 20, 50 or 100 mM (mean ± s.e.m.; n = 14–20 cells), using a similar protocol to that indicated above. All KCNK0 channel mutants retained the K^+ selectivity of the wild-type channel, as indicated by the expected dependence of the reversal potential of the mutant channels on the external K^+ concentration (not shown). For measurement of KCNK0 channel current blockage by Zn^{2+}, oocytes were held at –80 mV and current levels (mean ± s.d.; n = 4–7 cells) were monitored every 5 s at +20 mV before and during application of Zn^{2+} (0.1 nm to 1 mM) in 4 mM K^+ solution. To measure KCNK0 channel current blockage by Ba^{2+}, oocytes expressing wild-type or mutant KCNK0 channels were injected with 36 nl of 7.5 mM Ba^{2+} solution (internal Ba^{2+} concentration of ~250 μM). Following injection, the oocytes (n = 8–12) were held at –80 mV, and Ba^{2+}-induced current blockage was initiated by a depolarizing pulse to + 40 mV (because internally applied Ba^{2+} ions bind K^+ channels only at positive potentials). To eliminate Ba^{2+}-induced activation of chloride channels, the NaCl and KCl components of the bath solution (see above) were replaced with sodium and K^+ gluconate, respectively.

Unitary KCNK0 single-channel currents were recorded using a patch-clamp amplifier (Axopatch 200B, Molecular Devices) in the cell-attach configuration. Data were digitized at 20 kHz and filtered at 5 kHz (8-pole Bessel filter). Patch pipette resistance was 7–15 MΩ. The extracellular (bath) solution contained 140 mM KCl, 1.8 mM $CaCl_2$, 2 mM $MgCl_2$, 5 mM HEPES, pH 7.6, whereas the pipette solution contained 140 mM KCl, 1.8 mM $CaCl_2$, 2 mM $MgCl_2$, 5 mM HEPES, pH 7.6.

Data analysis. Voltage-activation curves were fitted, using the Origin program (version 5, Microcal Software), to a two-state Boltzmann equation: $I/I_{max} = (1 + \mathrm{EXP}(-ZF(V - V_{1/2})/RT))^{-1}$, where I/I_{max} is the normalized tail current amplitude of the *Shaker* channel, Z is the activation slope factor, $V_{1/2}$ is the half-activation voltage, T is the temperature in degrees kelvin and F and R are the Faradey and gas constants, respectively. Free-energy differences between closed (C) and open (O) states of the wild-type or mutant channels were parameterized based on gating shifts and slopes according to $\Delta G_{open} = (-RTln[O]/[C]) = ZFV_{1/2}$. Standard errors in ΔG_{open} were calculated by standard linear error propagation[33]. Time constants for current blockage by Zn^{2+} were calculated by fitting the data to the single exponential equation $I = I_0 + Ae^{-t/\tau}$, where I is the measured current, I_0 is the blocked current level at equilibrium, t is the elapsed time following zinc application, τ_{on} is the apparent time constant for current block and A is an amplitude constant. Dose-response data for Zn^{2+}-mediated blockage of wild-type or mutant KCNK0 currents were analyzed according the following reaction scheme $I_O \overset{K_C^I}{\longleftrightarrow} I_C + Zn^{2+} \overset{K_d}{\longleftrightarrow} I_C Zn^{2+}$, where K_C^I and K_d are the equilibrium constants for activation gate closure and Zn^{2+} binding to the closed conformation of the inactivation gate, respectively. Values for K_C^I and K_d were obtained by fitting the dose-response data to the following equation, derived based on the scheme above: $P_O = (1/(1+K_C^I(1+K_d/[Zn^{2+}])))$ (**Fig. 4d**). Time constants for Ba^{2+}-induced K^+ current blockage were derived upon fitting the data (**Fig. 5d**) to a double-exponential equation. The dominant time constant, as determined from the amplitudes of the two exponents, is reported. Open probability (P_O) of the wild-type or mutant KCNK0 channels was calculated using pClamp 9 software from five to eight single-channel recording traces (each along 5–10 min). The data were filtered as indicated, before analysis.

Note: Supplementary information is available on the Nature Structural & Molecular Biology website.

ACKNOWLEDGMENTS

We thank C. Deutsch for valuable comments and insight on this manuscript. O.Y. is the incumbent of the Belle and Murray Nathan Career Development Chair in Neurobiology. N.Z. is the incumbent of the Murray and Judith Shusterman Career Development Chair in Microbiology. This research was funded by grants from the Bi-national (US-Israel) Science Foundation (BSF) to O.Y., Y.Z and N.Z. (grant 2005112) and the Israel Science Foundation (ISF) grant to N.Z. (grant 431/03).

AUTHOR CONTRIBUTIONS

O.Y. and N.Z. designed the research; Y.B. performed the research; O.Y., N.Z. and Y.B. analyzed the data, Y.Z contributed new insights/analytical tools and O.Y. wrote the paper.

Published online at http://www.nature.com/nsmb/
Reprints and permissions information is available online at http://npg.nature.com/reprintsandpermissions/

1. Hille, B. *Ion Channels of Excitable Membranes* (Sinauer, Sunderland, MA, 2001).
2. Doyle, D.A. *et al.* The structure of the potassium channel: molecular basis of K^+ conduction and selectivity. *Science* **280**, 69–77 (1998).
3. Lu, Z., Klem, A.M. & Ramu, Y. Ion conduction pore is conserved among potassium channels. *Nature* **413**, 809–813 (2001).
4. MacKinnon, R., Cohen, S.L., Kuo, A., Lee, A. & Chait, B.T. Structural conservation in prokaryotic and eukaryotic potassium channels. *Science* **280**, 106–109 (1998).
5. Shealy, R.T., Murphy, A.D., Ramarathnam, R., Jakobsson, E. & Subramaniam, S. Sequence-function analysis of the K^+-selective family of ion channels using a comprehensive alignment and the KcsA channel structure. *Biophys. J.* **84**, 2929–2942 (2003).
6. Lesage, F. & Lazdunski, M. Molecular and functional properties of two-pore-domain potassium channels. *Am. J. Physiol. Renal Physiol.* **279**, F793–F801 (2000).
7. Goldstein, S.A., Bockenhauer, D., O'Kelly, I. & Zilberberg, N. Potassium leak channels and the KCNK family of two-P-domain subunits. *Nat. Rev. Neurosci.* **2**, 175–184 (2001).
8. Bezanilla, F. The voltage sensor in voltage-dependent ion channels. *Physiol. Rev.* **80**, 555–592 (2000).
9. Sigworth, F.J. Voltage gating of ion channels. *Q. Rev. Biophys.* **27**, 1–40 (1994).
10. Yellen, G. The moving parts of voltage-gated ion channels. *Q. Rev. Biophys.* **31**, 239–295 (1998).
11. del Camino, D., Holmgren, M., Liu, Y. & Yellen, G. Blocker protection in the pore of a voltage-gated K^+ channel and its structural implications. *Nature* **403**, 321–325 (2000).
12. Liu, Y., Holmgren, M., Jurman, M.E. & Yellen, G. Gated access to the pore of a voltage-dependent K^+ channel. *Neuron* **19**, 175–184 (1997).
13. Cordero-Morales, J.F. *et al.* Molecular determinants of gating at the potassium-channel selectivity filter. *Nat. Struct. Mol. Biol.* **13**, 311–318 (2006).
14. Hoshi, T., Zagotta, W.N. & Aldrich, R.W. Two types of inactivation in *Shaker* K^+ channels: effects of alterations in the carboxy-terminal region. *Neuron* **7**, 547–556 (1991).
15. Liu, Y., Jurman, M.E. & Yellen, G. Dynamic rearrangement of the outer mouth of a K^+ channel during gating. *Neuron* **16**, 859–867 (1996).
16. Loots, E. & Isacoff, E.Y. Protein rearrangements underlying slow inactivation of the *Shaker* K^+ channel. *J. Gen. Physiol.* **112**, 377–389 (1998).
17. Ogielska, E.M. *et al.* Cooperative subunit interactions in C-type inactivation of K channels. *Biophys. J.* **69**, 2449–2457 (1995).
18. Panyi, G., Sheng, Z. & Deutsch, C. C-type inactivation of a voltage-gated K^+ channel occurs by a cooperative mechanism. *Biophys. J.* **69**, 896–903 (1995).
19. Niemeyer, M.I. *et al.* Neutralization of a single arginine residue gates open a two-pore domain, alkali-activated K^+ channel. *Proc. Natl. Acad. Sci. USA* **104**, 666–671 (2007).
20. Zilberberg, N., Ilan, N. & Goldstein, S.A. KCNKO: opening and closing the 2-P-domain potassium leak channel entails "C-type" gating of the outer pore. *Neuron* **32**, 635–648 (2001).
21. Cohen, A., Ben-Abu, Y., Hen, S. & Zilberberg, N. A novel mechanism for human $K_{2P}2.1$ channel gating: facilitation of C-type gating by protonation of extra cellular histidine residues. *J. Biol. Chem.* **283**, 19448–19455 (2008).
22. Baukrowitz, T. & Yellen, G. Modulation of K^+ current by frequency and external K^+: a tale of two inactivation mechanisms. *Neuron* **15**, 951–960 (1995).
23. Baukrowitz, T. & Yellen, G. Use-dependent blockers and exit rate of the last ion from the multi-ion pore of a K^+ channel. *Science* **271**, 653–656 (1996).
24. Panyi, G. & Deutsch, C. Cross talk between activation and slow inactivation gates of *Shaker* potassium channels. *J. Gen. Physiol.* **128**, 547–559 (2006).
25. Panyi, G. & Deutsch, C. Probing the cavity of the slow inactivated conformation of *shaker* potassium channels. *J. Gen. Physiol.* **129**, 403–418 (2007).
26. Hoshi, T., Zagotta, W.N. & Aldrich, R.W. Biophysical and molecular mechanisms of *Shaker* potassium channel inactivation. *Science* **250**, 533–538 (1990).
27. Zagotta, W.N., Hoshi, T. & Aldrich, R.W. Restoration of inactivation in mutants of *Shaker* potassium channels by a peptide derived from ShB. *Science* **250**, 568–571 (1990).
28. Zilberberg, N., Ilan, N., Gonzalez-Colaso, R. & Goldstein, S.A. Opening and closing of KCNKO potassium leak channels is tightly regulated. *J. Gen. Physiol.* **116**, 721–734 (2000).
29. Schoppa, N.E. & Sigworth, F.J. Activation of *Shaker* potassium channels. III. An activation gating model for wild-type and V2 mutant channels. *J. Gen. Physiol.* **111**, 313–342 (1998).
30. Schoppa, N.E. & Sigworth, F.J. Activation of *shaker* potassium channels. I. Characterization of voltage-dependent transitions. *J. Gen. Physiol.* **111**, 271–294 (1998).
31. Zagotta, W.N., Hoshi, T. & Aldrich, R.W. *Shaker* potassium channel gating. III: evaluation of kinetic models for activation. *J. Gen. Physiol.* **103**, 321–362 (1994).
32. Zagotta, W.N., Hoshi, T., Dittman, J. & Aldrich, R.W. *Shaker* potassium channel gating. II: Transitions in the activation pathway. *J. Gen. Physiol.* **103**, 279–319 (1994).
33. Yifrach, O. & MacKinnon, R. Energetics of pore opening in a voltage-gated K^+ channel. *Cell* **111**, 231–239 (2002).
34. Jiang, Y. *et al.* The open pore conformation of potassium channels. *Nature* **417**, 523–526 (2002).
35. Armstrong, C.M. Voltage-gated K channels. *Sci. STKE* **2003**, re10 (2003).
36. Ding, S., Ingleby, L., Ahern, C.A. & Horn, R. Investigating the putative glycine hinge in *Shaker* potassium channel. *J. Gen. Physiol.* **126**, 213–226 (2005).
37. Lu, Z., Klem, A.M. & Ramu, Y. Coupling between voltage sensors and activation gate in voltage-gated K^+ channels. *J. Gen. Physiol.* **120**, 663–676 (2002).
38. Kitaguchi, T., Sukhareva, M. & Swartz, K.J. Stabilizing the closed S6 gate in the *Shaker* Kv channel through modification of a hydrophobic seal. *J. Gen. Physiol.* **124**, 319–332 (2004).
39. Proks, P., Antcliff, J.F. & Ashcroft, F.M. The ligand-sensitive gate of a potassium channel lies close to the selectivity filter. *EMBO Rep.* **4**, 70–75 (2003).
40. Magidovich, E. & Yifrach, O. Conserved gating hinge in ligand- and voltage-dependent K^+ channels. *Biochemistry* **43**, 13242–13247 (2004).
41. Carter, P.J., Winter, G., Wilkinson, A.J. & Fersht, A.R. The use of double mutants to detect structural changes in the active site of the tyrosyl-tRNA synthetase (*Bacillus stearothermophilus*). *Cell* **38**, 835–840 (1984).

42. Hidalgo, P. & MacKinnon, R. Revealing the architecture of a K^+ channel pore through mutant cycles with a peptide inhibitor. *Science* **268**, 307–310 (1995).
43. Horovitz, A. Double-mutant cycles: a powerful tool for analyzing protein structure and function. *Fold. Des.* **1**, R121–R126 (1996).
44. Aldrich, R.W. Inactivation of voltage-gated delayed potassium current in molluscan neurons. A kinetic model. *Biophys. J.* **36**, 519–532 (1981).
45. Aldrich, R.W., Jr, Getting, P.A. & Thompson, S.H. Mechanism of frequency-dependent broadening of molluscan neurone soma spikes. *J. Physiol. (Lond.)* **291**, 531–544 (1979).
46. Hsu, H. *et al.* Slow and incomplete inactivations of voltage-gated channels dominate encoding in synthetic neurons. *Biophys. J.* **65**, 1196–1206 (1993).
47. Loots, E. & Isacoff, E.Y. Molecular coupling of S4 to a K^+ channel's slow inactivation gate. *J. Gen. Physiol.* **116**, 623–636 (2000).
48. Gandhi, C.S., Loots, E. & Isacoff, E.Y. Reconstructing voltage sensor-pore interaction from a fluorescence scan of a voltage-gated K^+ channel. *Neuron* **27**, 585–595 (2000).
49. Gandhi, C.S., Clark, E., Loots, E., Pralle, A. & Isacoff, E.Y. The orientation and molecular movement of a K^+ channel voltage-sensing domain. *Neuron* **40**, 515–525 (2003).